Available online at www.sciencedirect.com
ScienceDirect
ELSEVIER
Polymer 47 (2006) 7425–7435
polymer
www.elsevier.com/locate/polymer

Counterion dependent crystallization kinetics in blends of a perfluorosulfonate ionomer with poly(vinylidene fluoride)

Eric P. Taylor, Forrest A. Landis, Kirt A. Page, Robert B. Moore*

Department of Polymer Science, The University of Southern Mississippi, 118 College Drive #10076, Hattiesburg, MS 39406-0001, USA

Received 9 June 2006; received in revised form 11 August 2006; accepted 11 August 2006
Available online 7 September 2006

Abstract

Blends of poly(vinylidene fluoride) (PVDF) with a perfluorosulfonate ionomer, Nafion®, have been prepared and examined in terms of the crystallization kinetics of the PVDF component. In blends of PVDF with Na^+-form Nafion®, the rates of bulk crystallization, as observed by DSC, and the spherulitic growth rates of the PVDF component, as observed using optical microscopy, were found to be very similar to that of pure PVDF. This behavior was attributed to the course phase separation of Na^+-form Nafion® from PVDF and melt incompatibility of the physically cross-linked ionomer with the crystallizable component. In this segregated state, the PVDF component of the blend is allowed to crystallize in pure phases that are isolated under the influence of Nafion®. In contrast, when the ionomer was exchanged with more weakly interacting quaternary alkylammonium counterions, a decrease in both the rate of bulk crystallization and spherulitic growth was observed. Furthermore, the crystallization kinetics of PVDF in these blends was found to be dependent on the counterion size; as the size of counterions associated with the Nafion® component increased, the rate of crystallization decreased. This behavior was attributed to a weakening of the electrostatic interactions in the ionomer phase and thus an increase in the extent of phase mixing with the larger ions.

Keywords: Crystallization kinetics; Nafion/PVDF blends; Counterion dependence

1. Introduction

Poly(vinylidene fluoride) (PVDF) is a semi-crystalline polymer that possesses a strong electric dipole moment associated with the C–F bonds in its monomer units; and consequently, PVDF is capable of interacting with a variety of polar polymers via dipole–dipole interactions [1–13]. In an attempt to utilize the tendency of PVDF to interact with polar polymers, several blend compatibility studies have been reported for blends of PVDF with a variety of ion-containing polymers [14]. Moussaif et al. investigated the miscibility of PVDF with poly(methyl methacrylate-*co*-zinc acrylate) ionomers [15] and polycarbonate grafted with poly(methyl methacrylate-*co*-zinc acrylate) [16]. These studies showed an increasing tendency toward miscibility with an increase in the ionic functionality of the ionomer. Linares et al. [17] showed that blends of PVDF and sulfonated polystyrene have improved compatibility and mechanical stability relative to control blends containing unmodified polystyrene. In a study directly relevant to this investigation, Kyu and Yang examined the phase behavior in blends of PVDF and Nafion® in the acid and sodium neutralized forms using small-angle laser light scattering (SALLS) [18,19]. These studies demonstrated that PVDF/Nafion® blends were partially compatible below the crystalline melting point of the PVDF component; however, liquid–liquid phase separation occurred when the blends were heated above the PVDF melting point.

In a more recent study involving the morphological characterization of PVDF in blends with a perfluorosulfonate ionomer (Nafion®) [20], we found that the nature of the Nafion® counterion can significantly affect the extent of phase separation of PVDF in this blend system. Using optical microscopic and scattering techniques, blends of Na^+-form Nafion® with PVDF were shown to exhibit a large degree of phase separation, which was attributed to the strong electrostatic forces

---

* Corresponding author. Tel.: +1 601 266 4480; fax: +1 601 266 5635.
E-mail address: rbmoore@usm.edu (R.B. Moore).

0032-3861/$ - see front matter © 2006 Elsevier Ltd. All rights reserved.
doi:10.1016/j.polymer.2006.08.023

involved within the ionic aggregates of the Nafion® ionomer. At temperatures above the melting point of PVDF, irreversible phase separation was observed. In these blends, the ionic aggregates act as electrostatic cross-links in the Nafion® rich phase thereby reducing the mobility of the ionomer chains and hindering the phase mixing with the PVDF component. However, when the Nafion® counterions in the blend with PVDF were exchanged from the strongly interacting Na^+ cations to larger alkylammonium counterions, i.e., tetrabutylammonium (TBA^+), a weakening of the electrostatic network allowed for a greater degree of phase mixing. At temperatures above the T_m of PVDF, the blend was found to be homogeneous and characteristic of a melt-miscible system.

For a polymer blend containing a crystallizable component, the extent of phase mixing can profoundly affect the crystallization behavior. Martuscelli has demonstrated that the rate of crystallization of semi-crystalline polymers in blends is greatly affected by the extent of phase mixing of the dispersed component [21]. In general, miscible polymer blends (i.e., where the polymer chains are mixed on a molecular level) will show the greatest decrease in the rate of crystallization due to a dilution of crystalline polymer at the crystal growth front and/or an increase in the glass transition temperature of the blend. The increase in the T_g of the blend is associated with a decrease in chain mobility near the crystallites, which hinders the diffusion of crystallizable segments to the crystal growth front, thereby reducing the rate of crystallization.

In blend systems which are not miscible on the molecular level (i.e., immiscible) and exhibit some degree of phase separation, Martuscelli has shown that the crystallization kinetics of the crystallizable component is dependent on the size of the dispersed domains [21]. In highly immiscible blends which exhibit strong phase separation (i.e., large phase-separated domains), the crystallizable component can crystallize in a manner virtually independent of the second blend component and no significant reduction in the rate of crystallization is observed relative to the pure homopolymer. Conversely, in blends containing dispersed domains that are small relative to the size scale of the developing crystalline domains, the growing crystals may reject, occlude and/or deform the phase-separated domains. This behavior generally reduces the crystal growth rate of the crystallizable component to a degree correlated with the size of the dispersed domain.

Based on our previous investigations on PVDF/Nafion® blends [20], the choice of counterion type may be used to control phase mixing and thus affect the crystallization kinetics of the PVDF component. In this study, we compare the phase behavior and crystallization kinetics of PVDF/Nafion® blends containing alkali metal ions to systems containing a series of alkylammonium ions of increasing size. By changing the counterion type and systematically varying the counterion size, the extent of phase mixing in these blends may be controlled by altering the electrostatic interactions in the Nafion® component. With a variety of blend morphologies at elevated temperatures (i.e., suitable crystallization temperatures for PVDF), ranging from a system with large-scale phase separation to a homogeneous, melt-miscible state, the influence of phase mixing on the crystallization kinetics of PVDF may be evaluated.

2. Experimental section

2.1. Materials

Poly(vinylidene fluoride) (Kynar® 720, $M_w = 140{,}000$ g/mol) was obtained from Atofina. Nafion® 117 (1100 equivalent weight, sulfonic acid form) was provided by E.I. DuPont de Nemours & Co. Alkylammonium hydroxides and sodium hydroxide were obtained from Aldrich Chemical Co. and used without further purification. All other solvents and reagents were obtained from Aldrich Chemical Co. and used without further purification.

2.2. Preparation of Nafion®/PVDF blends

Soluble powders of Na^+-, tetramethylammonium (TMA^+)-, tetraethylammonium (TEA^+)-, tetrapropylammonium (TPA^+)- and tetrabutylammonium (TBA^+)-neutralized Nafion® were prepared using previously described techniques [22]. The as-received, acid-form Nafion® membranes were refluxed in an 8 M methanolic sulfuric acid solution for 1 h to ensure complete conversion of the films to the acid neutralized form. The films were then washed several times in boiling water to remove excess acid. To convert the Nafion® membranes to the neutralized forms, the acid-form films were refluxed in a 1 M solution of the appropriate sodium or alkylammonium hydroxide in 50/50 methanol/water for 1 h. The resulting films were washed several times in boiling water and dried in a vacuum oven for 24 h at 80 °C. Gravimetric analysis confirmed that this neutralization procedure resulted in Nafion® membranes with greater than 95% neutralization of the sulfonic acid groups.

Using a Parr reactor [23], the neutralized Nafion® membranes were dissolved at 250 °C and ca. 1400 psi in a 50/50 ethanol/water solution for the Na^+-, TMA^+- and TEA^+-neutralized ionomer and in a 45/5/50 ethanol/2-propanol/water solution for the TPA^+- and TBA^+-neutralized ionomer sample. Two separate procedures were utilized to recover the perfluorosulfonate ionomers (PFSIs) from solution. The TPA^+- and TBA^+-form Nafion® samples were recovered by a "steam-stripping" process [22]. The solutions were slowly dripped into a large volume of boiling water, causing the organic solvents to rapidly evaporate, leaving a white, fluffy residue of the hydrophobic ionomer. The TPA^+ and TBA^+-form Nafion® residues were recovered, dried in a vacuum oven for 24 h at 80 °C and ground into a fine powder using a mortar and pestle. The Na^+-, TMA^+- and TEA^+-form Nafion® samples were recovered from solution by slowly evaporating the ionomer solutions at room temperature under a nitrogen purge. The ionomer residues were removed from the glass evaporation dish, dried in a vacuum oven at 80 °C for 24 h and ground into a powder using a mortar and pestle. Using these two techniques, all of the neutralized forms of Nafion® were amorphous and readily soluble in solvents such as dimethyl sulfoxide.

Solution blends of the Nafion® ionomers with PVDF were prepared by combining the powdered polymers in the proper weight fractions in glass vials and dissolving in dimethyl sulfoxide (DMSO) on a hot plate at 150 °C. Approximately 0.1 g of solid polymer mixtures were dissolved in 5 ml of dimethyl sulfoxide. Films for DSC and optical analysis were prepared using two different casting techniques. Thin films (ca. 2–10 μm in thickness) for optical analysis were prepared by casting the blend solutions onto glass slides on a hot plate at 150 °C, followed by vacuum drying at 80 °C for 24 h. Thicker films for DSC analysis were prepared by solution processing ca. 5 ml of the polymer solutions in 20 ml glass vials on a hot plate at 150 °C. After vacuum drying at 80 °C for 24 h, the resulting films had a thickness of 100–150 μm.

2.3. Dynamic mechanical analysis

Dynamic mechanical analysis was performed on pure Nafion® samples in all counterion forms to investigate the effect of counterion type and size on the dynamic mechanical properties. Dynamic mechanical measurements were performed using a Seiko Instruments SDM 5600 Series dynamic mechanical spectrometer (DMS 210). Samples were cut from the dry, neutralized membranes to dimensions of 1 cm × 5 cm × 0.2 mm and analyzed in the tensile mode at a frequency of 1 Hz and at a heating rate of 5 °C/min.

2.4. Small-angle laser light scattering analysis

The effect of the Nafion® counterion type on phase separation within Nafion®/PVDF blends was examined using a small-angle laser light scattering (SALLS) apparatus similar to that described by Stein and Rhodes [24]. Thin films of the polymer blends were cast onto microscope slides from a 1.5% (w/v) solution in DMSO resulting in a final film thickness of 2–3 μm. The microscope slides were placed in a Mettler FP82HT hot stage mounted on the sample holder in the SALLS setup. The incident light was produced from a 3 mW He–Ne laser with $\lambda = 632.8$ nm (Oriel® Corp., Model 6697), and the scattered V_v patterns were projected onto a paper film that could be moved in order to adjust the sample to detector distance. A digital image of the projected pattern was acquired using a Photometrics SenSys 1401E CCD area detector. The acquisition software was RSImage from Roper Scientific and the intensity of the scattering pattern as a function of pixel position was integrated using the POLAR® software package (SUNY Stonybrook).

2.5. Thermal analysis of bulk crystallization kinetics

The isothermal crystallization kinetics of the Nafion®/PVDF blends was examined using a Perkin Elmer Pyris 1 Differential Scanning Calorimeter. The mass of each of the blended films used in the DSC analysis was 15–20 mg. The thermal program of the DSC involved heating the samples to 220 °C for 5 min to remove any residual crystallinity of the PVDF component, followed by a rapid quench (ca. −200 °C/min) to the appropriate isothermal crystallization temperature. The samples were held at each crystallization temperature until completion of the exothermic crystallization event. For the PVDF resin chosen for this study, the lowest achievable isothermal crystallization temperature was found to be between 138 and 142 °C, and dependent on Nafion® concentration and counterion type. Isothermal crystallization at lower temperatures allowed for crystallization during the cooling process resulting in a final crystalline morphology which is not indicative of an isothermal process.

The resulting crystallization isotherms of the blends were analyzed using the Perkin Elmer software package to obtain plots of the fractional degree of crystallinity, X_c, versus time. These bulk crystallization isotherms were then analyzed using the Avrami approach [25,26]

$$\ln[-\ln(1 - X_c(t))] = \ln K + n \ln t \tag{1}$$

where t is the time of crystallization, K is the crystal growth rate constant and n is the Avrami exponent, which is related to the nucleation and growth mechanisms of the polymer crystallites. For this Avrami analysis, the linear region of the data, plotted in the form of Eq. (1), was set between the limits $X_c = 0.25$ and 0.75, where the spherulites of measurable radii grow with time in a linear, unperturbed manner (i.e., free of impingement and contributions from secondary crystallization).

2.6. Optical microscopic analysis of the spherulitic growth rate

The growth of the PVDF spherulites in the various blends with Nafion® was characterized using a Nikon Optiphot2 polarizing optical microscope with an attached Mettler FP82HT hot stage. The thin cast films (ca. 10 μm, prepared as described above) were heated to 220 °C for 5 min to remove any residual crystallinity and rapidly cooled (ca. 20 °C/min) to the appropriate isothermal crystallization temperature so as to observe the growth of individual spherulites. Images of spherulite growth during the crystallization of PVDF were obtained by a Nikon DXM1200 digital still camera mounted on the microscope. The diameters of at least three individual spherulites (of similar size and identical crystal form) were measured at several time intervals and averaged to obtain the growth rate of the spherulites.

3. Results and discussion

3.1. Effect of counterion type on the mechanical relaxation of Nafion®

Fig. 1 shows the dynamic mechanical behavior (plotted as $\tan\delta$ versus temperature) of Nafion® samples neutralized with Na^+, TMA^+, TEA^+, TPA^+ and TBA^+ counterions. For each of the alkylammonium neutralized Nafion® samples, two relaxations above 0 °C are clearly evident, and assigned as the α (high temperature peak) and β (low temperature

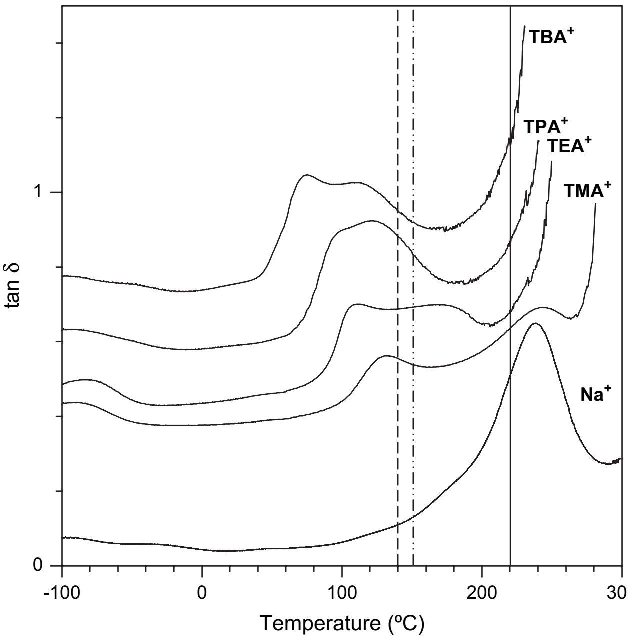

Fig. 1. Dynamic mechanical tan δ versus temperature plots for Na$^+$-, TMA$^+$-, TEA$^+$-, TPA$^+$- and TBA$^+$-form 1100 EW Nafion®. Curves are offset vertically for clarity.

peak) relaxations. For the Na$^+$-form sample, the dynamic mechanical behavior is dominated by the α relaxation observed at ca. 230 °C. In our recent studies [27,28], we have defined the molecular origins of these relaxations such that the α relaxation is attributed to the onset of long-range mobility of both the main- and side-chains facilitated by a profound weakening of the electrostatic interactions within the ionic aggregates. At temperatures in the vicinity of the α relaxation, a significant destabilization of the electrostatic network may be observed (i.e., through the activation of a *dynamic* network involving significant ion-hopping processes). In contrast, the β relaxation is assigned as the T_g of Nafion® associated with the onset of thermally activated main-chain motions that are facilitated through side-chain mobility within the framework of a *static* physical (electrostatic) network.

With an understanding of the effect of counterion size on chain dynamics and phase behavior in Nafion®, we are now able to correlate the impact of electrostatic interactions on the crystallization behavior of PVDF in blends with Nafion®. Included in Fig. 1 are markers indicating the important temperature regimes relevant to this study of the PVDF/Nafion® blends. The solid line indicates the annealing temperature, T_a, at which the blend samples were heated above the melting temperature of the PVDF component (T_m = ca. 180 °C) in order to eliminate the thermal history prior to the isothermal crystallization experiments (see below). The dashed and dash–dotted lines indicate the lower and upper limits of the isothermal crystallization temperatures used in this study, respectively. As will be discussed below, it is of particular importance to note the range of these crystallization temperatures relative to the specific thermal relaxations of the Nafion® component.

3.2. Phase behavior of Nafion®/PVDF blends

Using small-angle laser light scattering analysis, Kyu and Yang [18,19] showed that a halo in the SALLS pattern of acid-form Nafion®/PVDF blends developed immediately above the melting point of PVDF. This behavior was attributed to the phase separation of the blend components consistent with the latter stages of spinodal decomposition. Similarly, we have found that Na$^+$-form Nafion®/PVDF blends heated to temperatures above the PVDF melting point phase-separate and yield a scattering halo (attributed to phase separation) that increases in intensity and moves to smaller scattering angles with increasing temperature, implying that the dimensions of the phase-separated domains become larger through a phase coarsening process [20]. In contrast, TBA$^+$-form Nafion®/PVDF blends, with an identical thermal treatment, remain melt-miscible and show no evidence of phase separation upon cooling to room temperature. This behavior was attributed to the weakened electrostatic interactions and greater chain mobility of the TBA$^+$-form Nafion® which allowed for a more intimate mixture of the Nafion® and PVDF chains at elevated temperatures [20].

SALLS patterns of the 50:50 wt% Nafion®/PVDF blends, in all counterion forms, are shown in Fig. 2. Upon heating the Na$^+$-form Nafion®/PVDF blend to 220 °C for 5 min, a distinct scattering halo develops indicative of phase separation. A similar scattering behavior is observed for the TMA$^+$-form blend; however, the size of the scattering halo was larger and of lower intensity than that observed for the Na$^+$-form blend. This behavior suggests that the characteristic dimensions of the phase-separated domains in the TMA$^+$-form blend are somewhat smaller than that of the Na$^+$-form blend and that the extent of phase mixing is enhanced and/or the number of these smaller domains is less than in the Na$^+$-form blend. From the position of the scattering maxima, the average inter-domain distances for the Na$^+$ and TMA$^+$-form blends were found to be 25 μm and 13 μm, respectively. Since both the Na$^+$- and the TMA$^+$-forms of Nafion® exhibit high α relaxations (at temperatures greater than the annealing temperature of 220 °C), it is expected that the strong electrostatic interactions in these systems would yield a driving force for de-mixing through an irreversible gelation process of the Nafion® component [20]. Nevertheless, the distinct β relaxation observed with TMA$^+$-form Nafion® apparently yields sufficient mobility to slightly counteract the process of de-mixing at these elevated temperatures.

As the size of the alkylammonium counterion associated with the Nafion® component is increased, the intensity of the scattering halo decreases significantly. For the large counterions in the TPA$^+$- and TBA$^+$-form blends, a featureless scattering profile is exhibited with no evidence of a halo up to a temperature of 220 °C. It is apparent through this analysis that Na$^+$- and the TMA$^+$-forms of Nafion® are immiscible with PVDF and yield phase-separated domains with dimensions on the order of micrometers. With an organic counterion of intermediate size, as in the TEA$^+$-form Nafion® blend, a much higher mobility at 220 °C (T_α of 160 °C) apparently

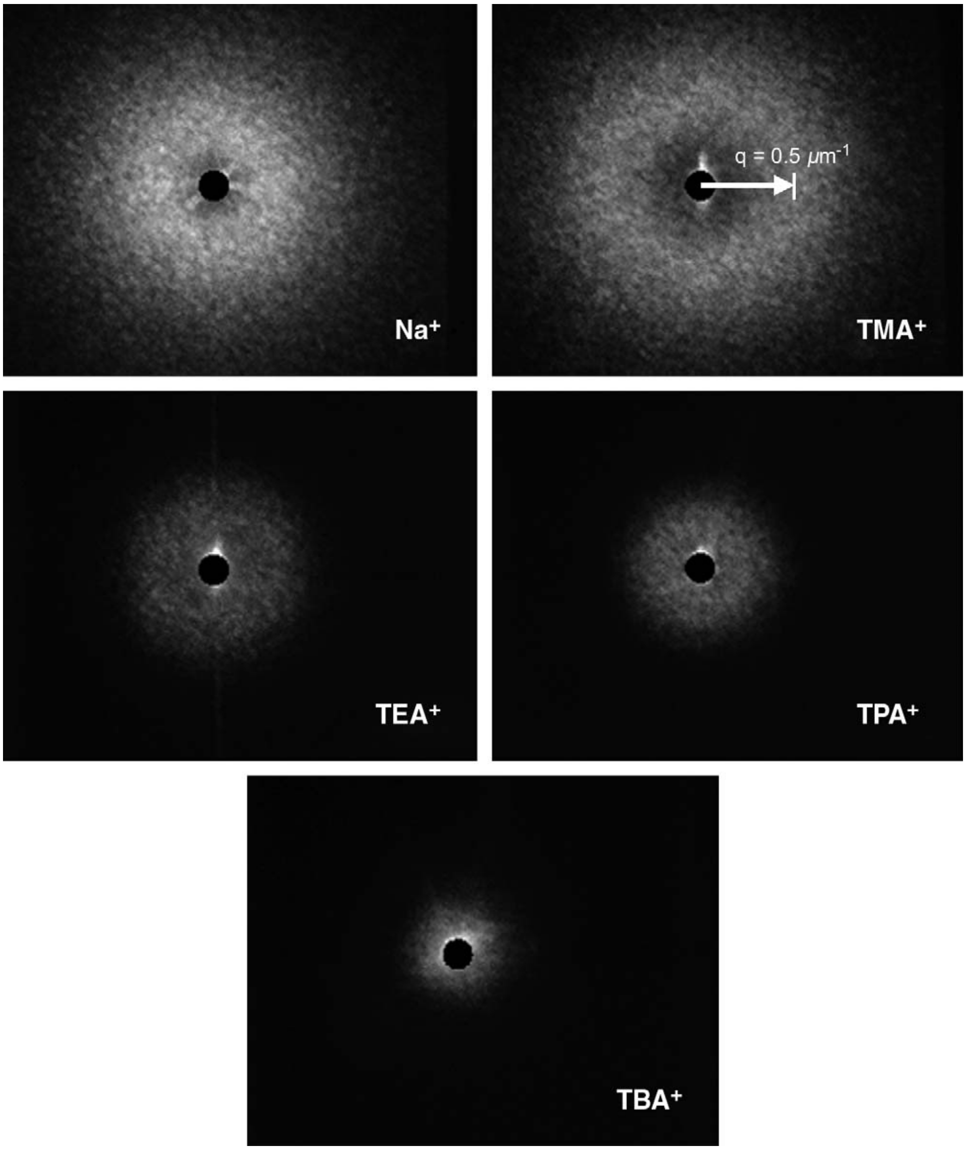

Fig. 2. Small-angle laser light scattering patterns of 50/50 Nafion®/PVDF blends held for 5 min at 220 °C. The scattering vector scale is the same for all patterns.

yields a more "melt-compatible" blend with PVDF (i.e., phase separated with significant phase mixing) and thus a very weak scattering halo at temperatures above the melting point of PVDF. For the large counterions, the rheological behavior of the Nafion® component becomes more liquid-like at 220 °C and the phase dimensions of the TPA$^+$- and TBA$^+$-form Nafion®/PVDF blends (if they exist) are not measurable or on a size scale below that which can be probed using SALLS. In agreement with our previous study, the TPA$^+$- and TBA$^+$-form Nafion®/PVDF blends are considered to be melt-miscible [20].

3.3. Bulk crystallization kinetics of Nafion®/PVDF blends

The results of bulk crystallization kinetics indicate that the nature of the Nafion® counterion has a significant effect on the crystallization kinetics of the PVDF blend component. Fig. 3 shows the DSC crystallization isotherms of a 50/50 blend composition of Na$^+$- and TBA$^+$-form Nafion® with PVDF at various isothermal crystallization temperatures. The isotherms of the 50/50 Na$^+$-form Nafion® blends with PVDF (Fig. 3a) show much shorter crystallization times in comparison with the isothermal data of the bulk crystallization rate of PVDF in the presence of TBA$^+$-form Nafion® (Fig. 3b). Dynamic mechanical studies of Na$^+$-form Nafion® show that the α relaxation, attributed to the onset of significant mobility within the ionic domains (i.e., a transition from a static network to a dynamic network), is found at a temperature of approximately 230 °C [22,27]. At temperatures associated with the "melt" of the blends (i.e., at 220 °C), the Na$^+$-form Nafion® is still electrostatically locked in a static network and is unable to phase mix with the PVDF component of the blend [20]. In contrast, the α relaxation in TBA$^+$-form Nafion® is found at a temperature of approximately 115 °C (Fig. 1), well below the temperature of the PVDF melt. This greatly

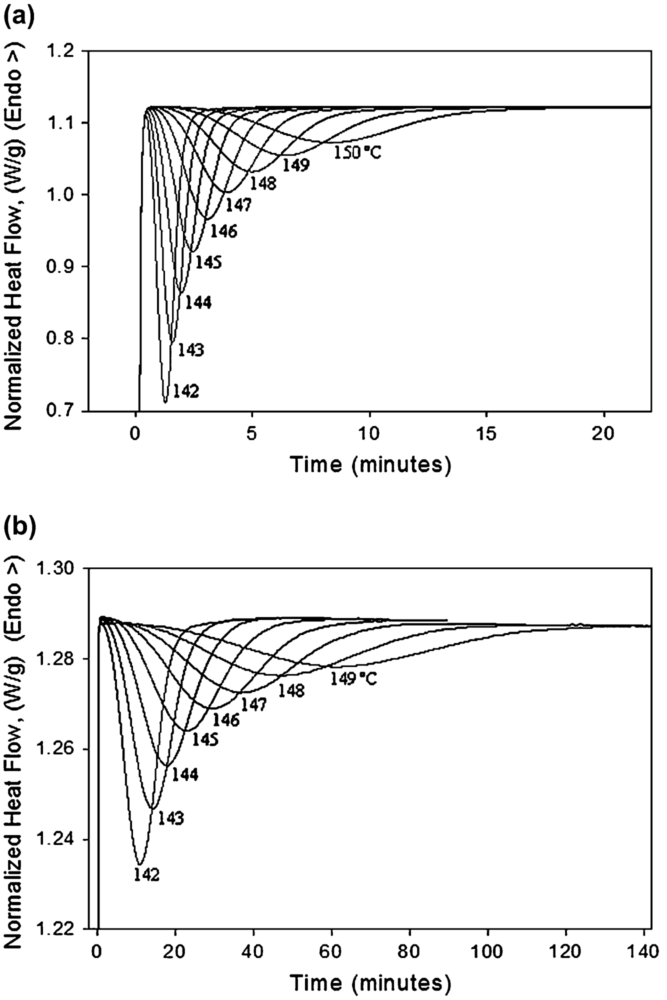

Fig. 3. Crystallization exotherms of 50/50 Nafion®/PVDF blends at various temperatures. (a) Na^+-form Nafion®/PVDF, (b) TBA^+-form Nafion®/PVDF.

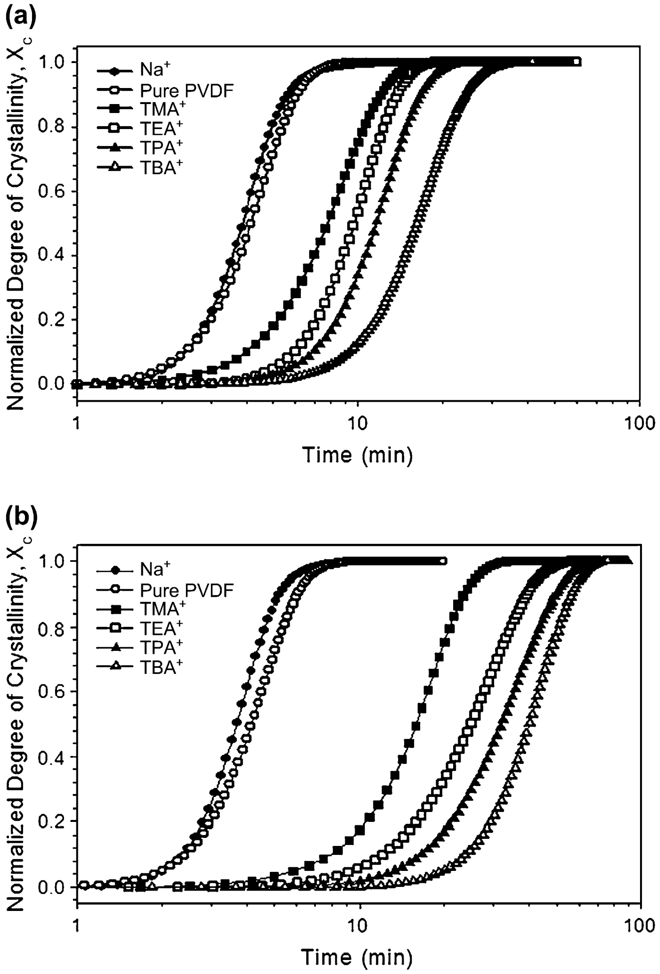

Fig. 4. Crystallization isotherms of PVDF and Nafion®/PVDF blends. (a) 20/80 Nafion®/PVDF, (b) 50/50 Nafion®/PVDF.

reduced α relaxation temperature is due to the weak electrostatic interactions between ion pairs containing the large, diffuse alkyl counterions and a potential plasticization effect from the bulky organic ions within the ionomer matrix. TBA^+-form Nafion® becomes a viscous liquid above this temperature allowing phase mixing with the molten state of PVDF. As a result of the intimate mixture of the Nafion® and PVDF chains in the melt, and the subsequent dilution of PVDF segments at the melt–crystal interface, the crystallization isotherms of 50/50 TBA^+-form Nafion® blends with PVDF display longer crystallization times indicating an overall decrease in the rate of crystallization of the PVDF component in this blend system.

In Fig. 4, the bulk crystallization isotherms for PVDF and five Nafion®/PVDF blends (20/80 blends in Fig. 4a and 50/50 blends in Fig. 4b) containing Na^+ ions and a range of alkylammonium counterions (TMA^+ through TBA^+) are plotted as the relative crystallinity versus time at 146 °C. These isotherms are useful in determining the crystallization half-times of a crystallizable sample (where $t_{1/2}$ is the time required for the samples to reach 50% of its maximum crystallinity) as well as determining the Avrami exponents and coefficients (discussed below). From these data, it is clear that the rate of PVDF crystallization decreases systematically with increasing counterion size in the Nafion® component, and as expected with an increase in the overall Nafion® composition in the blends. Furthermore, the uniform (superimposible) shape of the isotherms for all samples suggests that the mechanism of crystallization does not change significantly with blend composition or counterion type.

For the Na^+-form Nafion®/PVDF blends, it is important to note that the isotherms are quite comparable to that of pure PVDF. Again, this behavior is attributed to the distinct phase separation between the Na^+-form Nafion® and PVDF that occurs once the blend is heated above the melting point of PVDF. With this coarse phase separation, the PVDF component is able to crystallize in a state isolated from the Nafion® component. For the blends containing the alkylammonium counterions, the isotherms show a profound shift to longer times, with uniform progressions in time with increasing counterion size. As observed in the SALLS data of Fig. 2, the extent of phase separation decreases with increasing counterion size as the strength of the electrostatic interactions within the Nafion® component weakens. This behavior apparently allows for increased phase mixing with counterion size and thus the crystallization of the PVDF component becomes more intimately influenced by the mobility of the Nafion® chain segments in the melt. During crystallization, the growing PVDF crystallites must reject the small Nafion® domains or mobile chains from the crystal growth front resulting in a reduced crystal growth rate.

As the alkylammonium counterion size of Nafion® increases from the tetramethylammonium counterion through the tetrabutylammonium counterion, it is important to recall that the α relaxation (Fig. 1) decreases from 235 to 110 °C. Thus, after quenching the blends from 220 °C to the crystallization temperature, it is likely that the TMA^+ blend still contains small gel particles (in agreement with the data in Fig. 2), while the domains decrease in size and extent of phase mixing for the larger counterion systems. Consequently, it is likely that the retarded crystallization behavior for the alkylammonium ion series of blends progresses from a rejection of small domains (for the TMA^+-form Nafion®/PVDF blends) to a process involving the dilution of crystallizable PVDF segments at the crystal growth face by highly mobile TBA^+-form Nafion® chains. Depending on the extent of phase mixing, crystallization of the blends containing counterions of intermediate size may involve contributions from both processes.

The crystallization isotherms shown in Fig. 4 (and at each of the other isothermal crystallization temperatures) exhibit a sigmoidal shape which can be analyzed in terms of the Avrami equation [25,26]. The average Avrami exponents at each isothermal crystallization temperature, calculated from the analysis of the crystallization isotherms for PVDF and all Nafion® blends with PVDF at 146 °C, are summarized in Table 1. The value of each of the Avrami exponents for the blends of Nafion® with PVDF was within a close approximation of $n = 3$, indicating that crystallization of PVDF proceeds via three-dimensional growth and that the presence of Nafion® in the blend system does not significantly affect the nucleation mechanism of the PVDF component.

The crystal growth rate constants, K, derived from the Avrami analysis of the Nafion®/PVDF blends are also shown in Table 1 for a variety of Nafion®/PVDF blend compositions. For each blend composition, a progressive decrease in the magnitude of the crystallization rate constants is observed with an increase in counterion size. In addition, the rate constants generally decrease with increasing Nafion® content in the blends. An exception to this trend is observed for the Na^+-form Nafion®/PVDF blends, where the rate constants remain relatively constant and somewhat higher than that observed for pure PVDF. This contrast in behavior is attributed to the crystallization of PVDF in a coarsely phase-separated Na^+-form Nafion®/PVDF blend relative to that in a more phase mixed state, as observed for the blends containing alkylammonium counterions.

Bulk crystallization kinetics can be more thoroughly examined over a variety of blend compositions and crystallization temperatures by plotting the crystallization half-times, $t_{1/2}$, as a function of crystallization temperature (as shown in Fig. 5), where the magnitude of $t_{1/2}$ is an inverse measure of the overall rate of crystallization of the sample. It should be noted that the values of $t_{1/2}$ were obtained in the same temperature range for all counterion forms of the Nafion®/PVDF blends to enable better comparison between the counterion forms. The data in Fig. 5 are plotted for pure PVDF and all of the counterion forms of the Nafion®/PVDF blends at compositions of 20/80 (Fig. 5a) and 50/50 (Fig. 5b). For all of the samples and compositions, the crystallization half-times are observed to increase exponentially with T_c, characteristic of crystallization in the nucleation-controlled regime.

A comparison of the crystallization kinetics between pure PVDF and the Na^+-form Nafion®/PVDF system again demonstrates that the crystallization of PVDF is not greatly influenced by the presence of Na^+-form Nafion®. However, at high crystallization temperatures, the data in Fig. 5 indicate that Na^+-form Nafion® actually tends to accelerate the overall crystallization rate of the PVDF component. Although the molecular factors governing the kinetics of bulk crystallization involve contributions from both growth and nucleation, and the Na^+-form Nafion® components in these blends are presumably rather solid domains, it is most reasonable to expect that the accelerated crystallization behavior is attributed to an enhanced nucleation process. This phenomenon will be explored in further detail below.

When the counterion of the Nafion® component in the blend is changed from Na^+ to the alkylammonium counterions, a significant change is observed in the crystallization half-times of the PVDF blend component. TMA^+-Nafion®, which has an α relaxation centered at 230 °C, shows little evidence of phase mixing with PVDF through SALLS analysis (Fig. 2), but produces a noticeable reduction in the crystallization rate of PVDF especially at the high end of the crystallization window examined. With an increase in Nafion® content, there is a proportional increase in the crystallization half-times. By increasing the alkyl chain length of the counterion

Table 1
Avrami analysis of PVDF and Nafion®/PVDF blends at 146 °C

PVDF		Nafion® counterion	10/90 Nafion®/PVDF		20/80 Nafion®/PVDF		40/60 Nafion®/PVDF		50/50 Nafion®/PVDF	
K (min^{-1})	n		K (min^{-1})	n	K (min^{-1})	n	K (min^{-1})	n	K (min^{-1})	n
6.18	3.30	Na^+	–	–	8.61	3.63	7.12	3.22	7.89	3.65
		TMA^+	2.14	2.93	2.05	2.86	0.22	3.07	0.15	2.94
		TEA^+	1.90	3.10	1.60	3.10	0.16	2.95	0.08	2.64
		TPA^+	1.60	2.98	0.99	2.73	0.084	2.85	9.53e-3	2.73
		TBA^+	0.72	3.08	0.12	2.75	0.016	2.93	1.64e-3	2.90

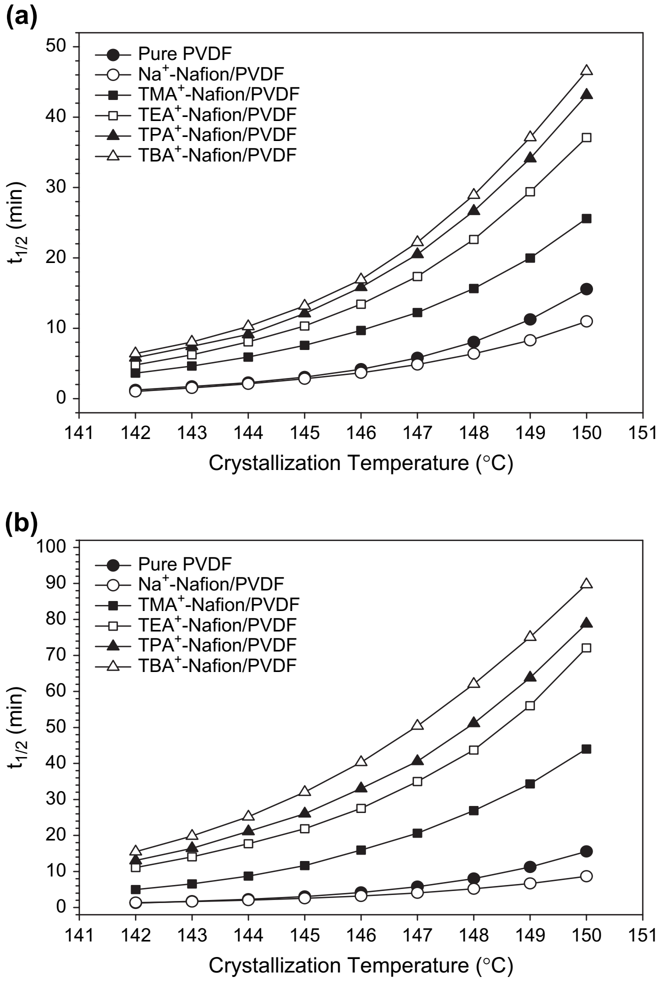

Fig. 5. Crystallization half-time of Nafion®/PVDF blends. (a) 20/80 Nafion®/PVDF, (b) 50/50 Nafion®/PVDF.

to TEA^+, the α relaxation of Nafion® drops to 160 °C, which is slightly above the temperature used as the crystallization window, but well below the T_m of PVDF. The expected viscous, liquid-like mobility of the TEA^+-form Nafion® component at the melt temperature of 220 °C allows increased phase mixing between Nafion® and PVDF. This condition significantly reduces the crystallization rate, and increases the crystallization half-time significantly compared to that of TMA^+-form Nafion® blends. An increase of the counterion size to TPA^+- and TBA^+-forms further increases the crystallization half-times, but to a lesser extent than the jump between TEA^+ and TMA^+.

All alkylammonium counterions larger than TMA^+ yield Nafion® α relaxations below that of the PVDF melt temperature, allowing for intimate phase mixing and a reduction in the bulk crystallization kinetics of PVDF. Since the size of the counterions principally affect the strength of electrostatic interactions in Nafion® [27], the most remarkable result of the data in Fig. 5 is that these interactions, which are specific to the non-crystallizable Nafion® component, are capable of imparting a high degree of control over the organization of the PVDF chain segments.

3.4. Spherulitic crystallization kinetics of Nafion®/PVDF blends

In order to further probe the influence of electrostatic interactions on the crystallization behavior of Nafion®/PVDF blends, the isothermal crystallization kinetics of the PVDF component may be evaluated by measuring the radial growth rate of the PVDF spherulites. The radial growth rate (G) of polymeric spherulites (obtained from the slope of the line acquired from plotting the experimental spherulitic radius versus time) can be described by the Turnbull–Fisher crystallization equation [29,30]

$$G = G_0 \exp\left(\frac{-\Delta F^*}{kT}\right)\exp\left(\frac{-\Delta \Phi^*}{kT}\right) \tag{2}$$

where the preexponential term G_0 is weakly temperature dependent and generally treated as a constant, T is the crystallization temperature, k is the Boltzmann's constant, ΔF^* is the activation energy for transport of the crystallizable chain segments across the liquid–crystal interface, and $\Delta \Phi^*$ is the free energy required to form a nucleus of critical size from the melt. Based on the analysis of Martuscelli [21], a non-crystallizable, melt-miscible component acts as a diluent that can influence both the transport term ΔF^* and the thermodynamic term $\Delta \Phi^*$ in Eq. (2). In the case where the T_g of the non-crystallizable component is greater than the T_g of the pure crystallizable component (as is the case for the Nafion®/PVDF blends in this study), ΔF^*(blend) will be greater than ΔF^*(cryst. comp.). The presence of the diluent also acts to increase the free energy of nucleation $\Delta \Phi^*$. Thus, the contribution of these two factors (separately or in combination) tends to depress the radial growth rate G in the compatible blend.

In the case of incompatible blends containing phase-separated domains of a non-crystallizable component, Martuscelli suggests that additional energies must be dissipated by the growing spherulites in order to reject, engulf, or deform these domains [21]. These additional energies are considered to constitute new energy barrier contributions to Eq. (2) that act collectively to depress the radial growth rate G in the incompatible blend. Of particular relevance to this study, the dependence of the growth rate G on the domain size of the dispersed phases was found to be quite strong, such that the finer the dispersion, the more pronounced the decrease in the growth rate.

Fig. 6 shows the isothermal growth rate of α-form spherulites in pure PVDF and PVDF in the presence of 50 wt% Nafion® neutralized in a variety of counterion forms. The growth rate of the PVDF spherulites in the presence of Na^+-form Nafion® is essentially the same as the growth rate of pure PVDF at low crystallization temperatures and is only slightly retarded at higher temperatures. This observation is consistent with that expected for a highly phase-separated blend morphology with PVDF crystallizing in a pure phase with little effect of the relatively large Na^+-form Nafion® domains. For the TMA^+-form Nafion®/PVDF blend, the system may be also classified as immiscible and phase separated (as shown by

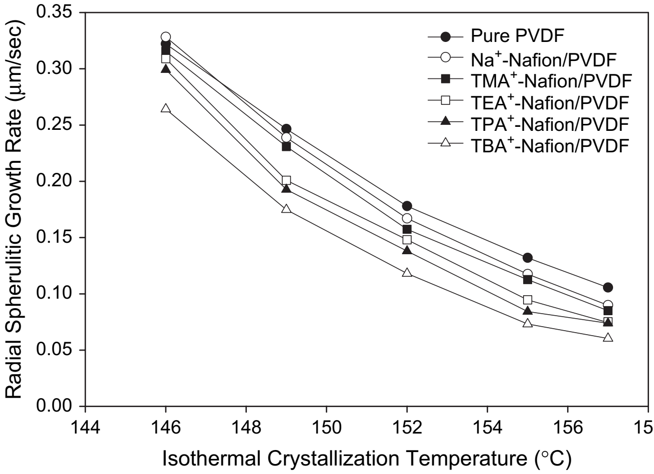

Fig. 6. Spherulitic growth rate of 50/50 Nafion®/PVDF blends.

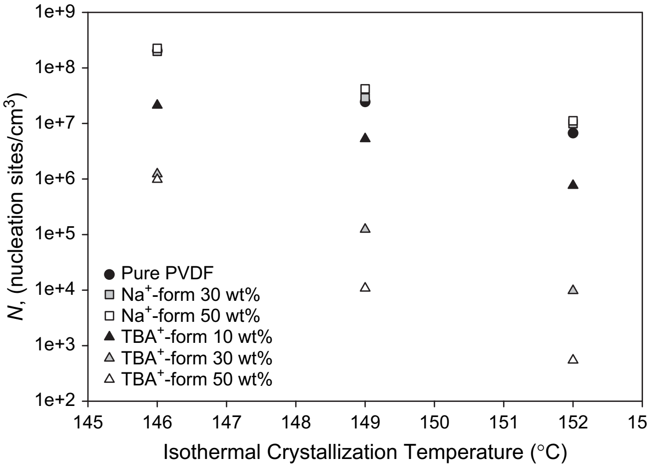

Fig. 7. Nucleation density, N, of PVDF, pure and blended, at various isothermal crystallization temperatures.

the SALLS results in Fig. 2); however, the domain sizes in this blend are smaller than that of the Na^+-form Nafion®/PVDF blend and thus the suppression of G is more distinct [21].

In contrast to the clearly immiscible Na^+ and TMA^+-form Nafion®/PVDF blends, the incorporation of the larger alkylammonium forms of Nafion® in the blends causes a significant decrease in the spherulitic growth rate as the size of the alkylammonium counterion increases. This observation suggests that due to the greater degree of phase mixing found in these alkylammonium-form Nafion®/PVDF blends (with the greatest phase mixing observed in the TBA^+-form Nafion®/PVDF blends) the growth of the PVDF spherulites is retarded by either a dilution of crystallizable segments at the crystal growth front or a rejection of very small domains (as would be undetectable with SALLS) from the crystal–melt interface.

Since the measurement of spherulitic crystallization kinetics provides quantitative information concerning the crystal growth process [31,32], while the bulk crystallization kinetics stems from contributions of both growth and nucleation [25,26,33,34], the complementary combination of these data sets may be used to separately evaluate the important contribution of nucleation in these blends. With knowledge of the Avrami rate constant, K, from the analysis of bulk crystallization kinetics, and the spherulitic growth rate, G, the nucleation density, N, at a specific crystallization temperature may be estimated by

$$N = \frac{3K}{4\pi G^3} \tag{3}$$

assuming that nucleation results in the formation of three-dimensional spherulites and that the increase in crystal dimensions is linear with crystallization time [1].

Fig. 7 shows the variation of the nucleation density of the PVDF component within Na^+- and TBA^+-form Nafion®/PVDF blends crystallized over a range of temperatures. For all samples, the nucleation density, N, is observed to decrease with an increase in the crystallization temperature (as expected for crystallization in the nucleation-controlled regime). For the Na^+-form Nafion®/PVDF blends, the incorporation of 30 and 50 wt% Na^+-form Nafion® in blends with PVDF had little effect on the nucleation density compared to the pure PVDF homopolymer (perhaps only a slight increase in N compared to PVDF). This relative independence of the nucleation density with blend composition yields further evidence that PVDF is crystallizing in a distinctly different phase from the Nafion® domains, and thus the crystallization behavior is basically that expected for pure PVDF domains. While the slight increase in nucleation density in the Na^+-form Nafion®/PVDF blends is essentially negligible in this data set, it is important to note that in blends containing very low levels of Na^+-form Nafion® (e.g., 1–10 wt%), the extremely small Nafion® domains actually act as efficient sites for nucleation and thus significantly enhance the PVDF nucleation density [35].

In contrast to the Na^+-form Nafion®/PVDF blends, addition of TBA^+-form Nafion® to PVDF substantially reduces the nucleation density by several orders of magnitude as compared to pure PVDF. Moreover, this effect is strongly dependent on composition and becomes more pronounced with increases in the Nafion® content and with the crystallization temperature.

With respect to counterion type, the nucleation density decreases with increasing counterion size, and is attributed to a weakening of the electrostatic interactions in the melt. Fig. 8 shows optical micrographs of pure PVDF and 50/50 Nafion®/PVDF blends in all 5 neutralized counterion forms isothermally crystallized at 146 °C for 30 min. PVDF (Fig. 8a) and the 50/50 Na^+-form Nafion®/PVDF blend (Fig. 8b) are found to be completely volume-filled at 146 °C after periods of 9 min and 7 min, respectively. Nucleation was observed to occur very rapidly in both of these systems with almost exclusive crystallization into the strongly birefringent, kinetically favored α crystal form [36]. The TMA^+-form blend (Fig. 8c) has a crystallization half-time of 15.7 min, which results in approximately 95% of the total crystallization achievable in the sample after isothermal crystallization for 30 min. The optical texture of the spherulites in this sample is also consistent with the predominant development of the α crystal form.

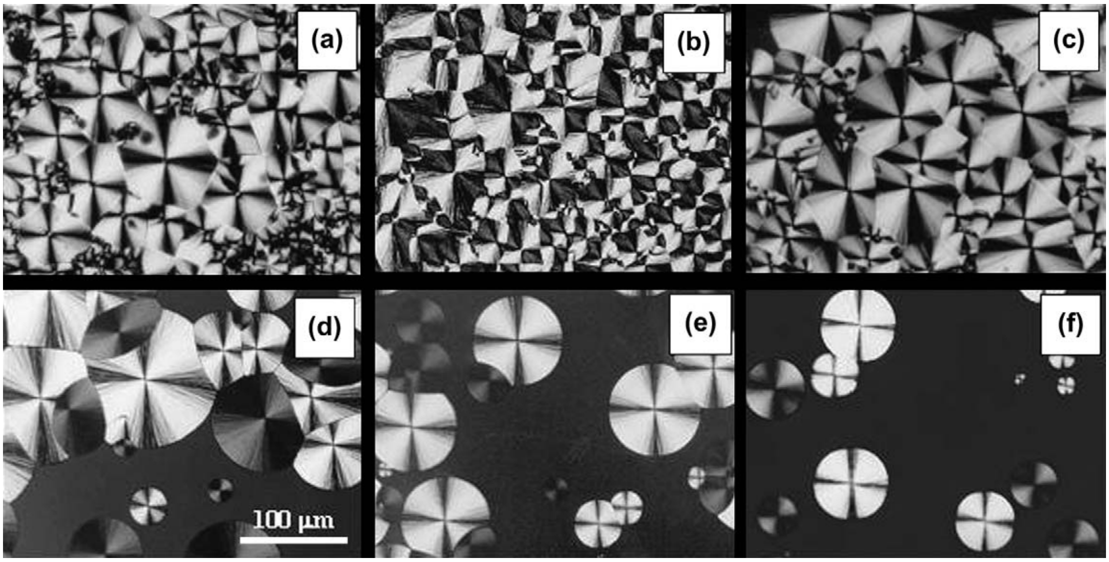

Fig. 8. PVDF and Nafion®/PVDF blends isothermally crystallized at 146 °C for 30 min. (a) Pure PVDF, (b) 50/50 Na^+-form Nafion®/PVDF, (c) 50/50 TMA^+-form Nafion®/PVDF, (d) 50/50 TEA^+-form Nafion®/PVDF, (e) 50/50 TPA^+-form Nafion®/PVDF, and (f) 50/50 TBA^+-form Nafion®/PVDF.

For the blends containing TEA^+-, TPA^+- and TBA^+-form Nafion®, the relatively long crystallization half-times of 26.4 min, 33.8 min and 41.6 min, respectively, yield samples that are not volume-filled after 30 min. Nucleation and spherulitic growth rates of PVDF in these systems gradually decrease as the size of the alkylammonium counterion increases. In addition, the inhibited growth rates facilitate the partial formation of the more thermodynamically favored γ crystal form (i.e., the weakly birefringent spherulites) [36]. This behavior is attributable to an increase in the degree of phase mixing between the blend components with counterion size, which drastically reduces the ability of the PVDF component to rapidly develop stable nuclei due to a dilution of the crystallizable PVDF chains in the melt. With the largest counterion form, the greatly diminished nucleation density yields further support for the recognition of TBA^+-form Nafion®/PVDF blends as a truly melt-miscible system [20].

4. Conclusions

In blends of PVDF with a perfluorosulfonate ionomer, such as Nafion®, the nature of the neutralizing counterion can have a significant effect on the crystallization behavior of the PVDF component. Using Avrami analysis of isothermal crystallization DSC data, the bulk crystallization rate of PVDF in the presence of Na^+-form Nafion® was shown to be comparable to the crystallization rate of pure PVDF homopolymer. Similarly, the spherulitic growth rate and the polymorphic composition of the resulting crystalline phase were found to be virtually identical to that of pure PVDF. Using SALLS, these blends were observed to be immiscible and phase separated in the melt state. Therefore, the crystallization behavior observed for these immiscible Na^+-form Nafion®/PVDF blends was attributed to the highly phase-separated blend morphology, which allowed the PVDF component to organize in a pure state free of the influences of the electrostatically cross-linked Nafion® component.

In contrast, blends of PVDF with alkylammonium-form Nafion® displayed a dramatic decrease in the bulk crystallization rates of the PVDF blend component relative to pure PVDF. Furthermore, this effect was observed to be systematically dependent on the size of the alkylammonium counterion. With an increase in the counterion size or the content of the Nafion® component, the rate of crystallization (bulk and spherulitic) decreased. By reducing the strength of the electrostatic network through the use of large organic cations, an increase in the melt-flow characteristics of Nafion® can occur at elevated temperatures. This increase in the mobility of the polymer chains within the ionomer allows for a greater degree of phase mixing with the PVDF blend component. Thus, the reduction in the rate of crystallization of PVDF in the presence of alkylammonium-form Nafion® was attributed to the greater degree of phase mixing, which caused the growing PVDF crystallites to reject the small domains or chains of the Nafion® blend component from the crystal growth front. As the size of the alkylammonium counterion increased, the blends became more compatible, shifting from an immiscible system with relatively small Nafion® domains (e.g., with the TMA^+-form Nafion® blends) to a melt-miscible system (e.g., with the TBA^+-form Nafion® blends). In agreement with the work of Martuscelli [21], this shift in blend morphology/miscibility with changes in electrostatic interactions results in a slowing of the overall crystallization rate due to the presence of small solid domains at the melt–crystal interface (for the immiscible systems) and due to a dilution of the crystallizable chains at the growth face (for the melt-miscible system).

The crystallization behavior of the Nafion®/PVDF blends was also shown to be defined by the interplay of nucleation density and the variation of the spherulitic radial growth rates of the spherulites at different isothermal crystallization temperatures and concentrations of the Nafion® component. The nucleation density of the blends was calculated by combining the spherulitic growth rate results obtained through polarized optical microscopy with the crystallization rate constant obtained through Avrami analysis of DSC isothermal experiments. The spherulitic growth rate of PVDF in blends with Nafion® was also shown to be affected by the type of counterion of the Nafion® blend component. Na^+-form Nafion® caused no significant change in the nucleation density or the spherulitic growth rate of the PVDF component indicating that this blend system was highly immiscible. In contrast, the nucleation density and the spherulitic growth rate of PVDF in blends with TBA^+-form Nafion® were significantly reduced relative to pure PVDF. As in the bulk crystallization results, the developing PVDF crystallites must form and grow by rejecting the TBA^+-form Nafion® chains from the crystal growth front, which consequently inhibits the formation of stable nuclei and lowers the growth rate of the resulting spherulites.

Acknowledgements

The authors would like to acknowledge DuPont for providing the Nafion® membranes. This work was partially supported by the MRSEC Program of the National Science Foundation under Award Number DMR 0213883, and Mississippi NSF EPSCoR program. Additional support for this work was provided by the American Society for Engineering Education; National Defense Science and Engineering Graduate Fellowship.

References

[1] Schneider S, Drujon X, Wittmann JC, Lotz B. Polymer 2001;42:8799.
[2] Fujita K, Kyu T, St. John Manley R. Macromolecules 1996;29:91.
[3] Liu L-Z, Chu B, Penning JP, St. John Manley R. Macromolecules 1997;30:4398.
[4] Huang J, Marand HL. Macromolecules 1997;30:1069.
[5] Bernstein RE, Cruz CA, Paul DR, Barlow JW. Macromolecules 1977; 10:681.
[6] Wahrmund DC, Bernstein RE, Barlow JW, Paul DR. Polym Eng Sci 1978;18:677.
[7] Nishi T, Wang T. Macromolecules 1975;8:909.
[8] Wang B, Nishi T. Macromolecules 1977;10:421.
[9] Liu ZH, Marechal P, Jerome R. Polymer 1997;38:5149.
[10] Liu ZH, Marechal P, Jerome R. Polymer 1996;37:5317.
[11] Bernstein RE, Wahrmund DC, Barlow JW, Paul DR. Polym Eng Sci 1978;18:1220.
[12] Reckinger C, Rault J. Rev Phys Appl 1986;21:11.
[13] Leonard C, Halary JL, Monnerie L. Polymer 1985;26:1507.
[14] Leung LM, Lo KKC. Polym Int 1995;36:339.
[15] Moussaif N, Jerome R. Polymer 1999;40(24):6831.
[16] Moussaif N, Pagnoulle C, Jerome R. Polymer 2000;41:5551.
[17] Canovas MJ, Acosta JL, Linares A. Revista de Plasticos Modernos 2000;79:64.
[18] Kyu T, Yang JC. Macromolecules 1990;23:176.
[19] Yang JC, Kyu T. Macromolecules 1990;23:182.
[20] Landis FA, Moore RB. Macromolecules 2000;33:6031.
[21] Martuscelli E. Polym Eng Sci 1984;24:563.
[22] Moore RB, Cable KM, Croley TL. J Membr Sci 1992;75:7.
[23] Martin CR, Rhoades TA, Ferguson JA. Anal Chem 1982;54:1639.
[24] Stein RS, Rhodes MB. J Appl Phys 1960;31:1873.
[25] Avrami M. J Chem Phys 1939;7:1103.
[26] Avrami M. J Chem Phys 1940;8:212.
[27] Page KA, Cable KM, Moore RB. Macromolecules 2005;38:6472.
[28] Page KA, Landis FA, Phillips AK, Moore RB. Macromolecules 2006; 39:3939.
[29] Turnbull D, Fisher JC. J Chem Phys 1949;17:71.
[30] St-Jean G, Barreto MC, Brown GR. Polym Eng Sci 1990;30:1098.
[31] Hoffman JD, Davis GT, Lauritzen JI. In: Hannay NB, editor. Treatise on solid state chemistry, vol. 3. New York: Plenum Press; 1976 [chapter 7].
[32] Hoffman JD, Miller RL. Polymer 1997;38:3151.
[33] Ravindranath K, Jog JP. J Appl Polym Sci 1993;49:1395.
[34] Page KA, Schilling GD, Moore RB. Polymer 2004;45:8425.
[35] Taylor EP. Ph.D. Dissertation, The University of Southern Mississippi; 2002.
[36] Lovinger AJ. J Polym Sci Polym Phys Ed 1980;18:793.